Strathprints Institutional Repository

Molecular Biology of the Cell
Vol. 17, 2035–2045, April 2006

Interacting Protein Kinases Involved in the Regulation of Flagellar Length

Maja Erdmann,* Anne Scholz,* Inga M. Melzer, Christel Schmetz, and Martin Wiese

Bernhard Nocht Institute for Tropical Medicine, Parasitology Section, D-20359 Hamburg, Germany

Submitted October 24, 2005; Revised December 29, 2005; Accepted January 26, 2006
Monitoring Editor: J. Silvio Gutkind

A striking difference of the life stages of the protozoan parasite *Leishmania* is a long flagellum in the insect stage promastigotes and a rudimentary organelle in the mammalian amastigotes. LmxMKK, a mitogen-activated protein (MAP) kinase kinase from *Leishmania mexicana*, is required for growth of a full-length flagellum. We identified LmxMPK3, a MAP kinase homologue, with a similar expression pattern as LmxMKK being not detectable in amastigotes, up-regulated during the differentiation to promastigotes, constantly expressed in promastigotes, and shut down during the differentiation to amastigotes. *LmxMPK3* null mutants resemble the *LmxMKK* knockouts with flagella reduced to one-fifth of the wild-type length, stumpy cell bodies, and vesicles and membrane fragments in the flagellar pocket. A constitutively activated recombinant LmxMKK activates LmxMPK3 in vitro. Moreover, LmxMKK is likely to be directly involved in the phosphorylation of LmxMPK3 in vivo. Finally, LmxMPK3 is able to phosphorylate LmxMKK, indicating a possible feedback regulation. This is the first time that two interacting components of a signaling cascade have been described in the genus *Leishmania*. Moreover, we set the stage for the analysis of reversible phosphorylation in flagellar morphogenesis.

INTRODUCTION

Protein kinases are central molecules in differentiation, proliferation, stress response, and apoptosis in all eukaryotic cells. A commonly used signaling pathway is that of the mitogen-activated protein (MAP) kinases. Its core module is comprised of a MAP kinase kinase kinase (MKKK), a MAP kinase kinase (MKK), and a MAP kinase. An external signal is sensed by a cell surface receptor, which subsequently undergoes autophosphorylation and recruits first intracellular signaling molecules. These can activate MKKK, which phosphorylates and activates its substrate MKK. MKKs are dual specificity kinases that activate their substrates, the MAP kinases, by phosphorylation on a threonine and tyrosine residue of the TXY motif in the activation lip region. Finally, MAP kinases can phosphorylate transcription factors, directly influencing the expression of certain genes, or they phosphorylate other soluble kinases or structural proteins of the cell. This is a very simplistic view of the processes occurring in a cell after stimulation, because there are among other proteins, a number of scaffold proteins involved that are responsible for the specificity of the phosphorelay. Moreover, protein phosphatases counterbalance the activity of the protein kinases by dephosphorylation.

One aspect of differentiation is the regulation of organelle and overall cell size. Flagellar length regulation is a simple one-dimensional example for maintenance of a defined size of an organelle, the flagellum. A flagellum is a dynamic structure that is built by the assembly of its components at its tip, which is also the site for the disassembly of the structural elements. The building blocks are delivered and removed by a process called intraflagellar transport (IFT). The balance between anterograde (base to tip) and retrograde IFT has been found to determine the length of the flagellum in the green alga *Chlamydomonas reinhardtii* (Marshall and Rosenbaum, 2001). It is likely, however, that protein phosphorylation adds an additional layer to the regulation of flagellar maintenance because >80 flagellar components have been found to be phosphorylated in *Chlamydomonas* (Piperno and Luck, 1976; Piperno *et al*., 1981; Harper *et al*., 1993; Tuxhorn *et al*., 1998). Our studies of the protozoan parasite *Leishmania* have shown that this parasite is a suitable model organism for flagellar length regulation because protein kinases of the MAP kinase signal transduction cascades are critically involved in its regulation (Wiese *et al*., 2003a; Bengs *et al*., 2005). Likewise, in *Chlamydomonas* LF4, a protein kinase with homology to MAP kinases and the human male germ cell-associated kinase (MAK), has been found to influence flagellar length as a null mutant displayed elongated flagella (Berman *et al*., 2003).

Leishmania parasites have a digenetic life cycle with the sandfly as their insect vector and mammals as their host. The insect stage promastigotes are spindle-shaped cells, 11–20 μm in length and 2 μm in diameter, with a long flagellum protruding from the flagellar pocket, an invagination of the cytoplasmic membrane at the anterior end of the cell. They are transmitted to a mammalian host during the bloodmeal of the sandfly. In the skin of the host, the promastigotes are taken up by macrophages and end up in the lysosome of the host cell, forming the parasitophorous vacuole. Instead of being killed and degraded, triggered by the elevated temperature and the low pH (Zilberstein and Shapira, 1994), the

This article was published online ahead of print in *MBC in Press* (http://www.molbiolcell.org/cgi/doi/10.1091/mbc.E05–10–0976) on February 8, 2006.

* These authors contributed equally to this work.

Address correspondence to: Martin Wiese (martin.wiese@bni-hamburg.de).

Abbreviations used: IFT, intraflagellar transport; MAP, mitogen-activated protein; PFR, paraflagellar rod.

parasites differentiate into the spherical amastigote form, which has an overall reduced cellular volume reflected by a length and width of 5–6 μm, a rudimentary flagellum not protruding from the flagellar pocket, and a different cell surface architecture (McConville and Ferguson, 1993). How the signals, a shift in temperature and in pH, are sensed and translated into differentiation is not known yet. However, it is likely that protein kinases and phosphatases play major roles because early investigations on phosphorylation patterns in different life stages of trypanosomatids revealed stage-specific changes in overall protein phosphorylation (Mukhopadhyay *et al*., 1988; Aboagye-Kwarteng *et al*., 1991; Parsons *et al*., 1991, 1993, 1995; Dell and Engel, 1994).

Using deletion analysis, we found that LmxMPK9 is involved in flagellar length regulation (Bengs *et al*., 2005). A null mutant displayed significantly elongated flagella compared with wild-type promastigotes. Flagellar length was also affected in a deletion mutant for the MAP kinase kinase LmxMKK (Wiese *et al*., 2003a). These mutants displayed flagella reduced to one-fifth of the length of the wild-type flagellum, preventing the cells from swimming free in the culture medium.

Here, we analyze LmxMPK3, which is encoded by the only MAP kinase gene investigated so far showing mRNA levels significantly down-regulated in the amastigote stage of *Leishmania mexicana* (Wiese *et al*., 2003b). We prove the kinase activity of LmxMPK3 by in vitro kinase assays of the recombinant protein expressed in *Escherichia coli*. Independently obtained homozygous deletion mutants of *LmxMPK3* display flagella significantly reduced in length resembling those of the *LmxMKK* null mutant (Wiese *et al*., 2003a). Indeed, the constitutively active LmxMKK phosphorylates and activates LmxMPK3 in vitro and in vivo.

MATERIALS AND METHODS

Parasites

Promastigotes of *L. mexicana* MNYC/BZ/62/M379 were grown as described previously (Menz *et al*., 1991). Female BALB/c mice were infected into the left hind foot pad at the age of 6–8 wk with 1×10^7 promastigote parasites in 30 μl of phosphate-buffered saline (PBS) (137 mM NaCl, 2.7 mM KCl, 8 mM Na_2HPO_4, and 1.4 mM KH_2PO_4). Using a caliper gauge, the course of infection was followed by measuring lesion size relative to the uninfected right hind foot pad at 4- to 5-wk intervals. For axenic amastigotes, cultures were seeded with stationary phase promastigotes at 4×10^6 cells/ml in Schneider's *Drosophila* medium (PAN Biotech, Aidenbach, Germany) supplemented with 20% inactivated fetal calf serum and 2 mM glutamine, adjusted to pH 5.5 by the addition of morpholinoethane sulfonic acid, and incubated at 34°C, 5% CO_2. Samples of 1×10^8 cells were taken at defined intervals after initiation of differentiation. For amastigote-to-promastigote differentiation, parasites were isolated from lesions of infected BALB/c mice as described previously (Wiese, 1998). The whole cell suspension was centrifuged for 10 min at 150 × *g* and 4°C. Then, the supernatant was centrifuged for 10 min at 1500 × *g* at 4°C. The pellet was resuspended in 10 ml of cold 1× PBS, and the cells were counted. One hundred milliliters of prewarmed (27°C) SDM-79 medium (Brun and Schoenenberger, 1979) was inoculated with 10^9 amastigotes. Every 5 h, cell pellets of 1×10^8 cells were collected, washed with cold 1× PBS, frozen in liquid nitrogen, and stored at −70°C.

Molecular Cloning Methods

Expand High-Fidelity Polymerase (Roche Diagnostics, Mannheim, Germany) was used for all PCR applications. Plasmid isolation, DNA/RNA isolation and blotting, and hybridizations were performed as described previously (Benzel *et al*., 2000). Both DNA strands of all constructs derived from PCR were verified by DNA sequencing. *LmxMPK3* sequence data have been submitted to DDBJ/EMBL/GenBank databases under accession no. AJ293281. Splice-addition sites were determined as described previously (Wiese, 1998) using the mini-exon–derived oligonucleotide 5′-CTAACGCTATATAAGTATCAGTTT-3′ and two oligonucleotides derived from *LmxMPK3*, 5′-CTTCGAAGCTGTGGTATT-3′ and 5′-GTCGCGACACTTCTTGAT-3′, as primers in the reverse transcriptase and polymerase chain reactions.

Antibody Production and Immunoblotting

A rabbit antiserum was produced against the peptide CTAGGSSSKNGSGHHH corresponding to the 15-COOH-terminal amino acids of LmxMPK3 (Eurogentec, Seraing, Belgium) and purified on the peptide. Lysates of 1×10^9 cells ml^{-1} in 1× lysis buffer (1× PBS, 0.1% SDS, 50 mM dithiothreitol, 50 μM leupeptin, 25 μM *N*-α-p-tosyllysyl-chloromethylketone, 1 mM phenylmethylsulfonyl fluoride, 10 mM 1,10-phenanthroline, and 1× SDS sample buffer [0.4% SDS, 4% glycerol, 0.0002% bromphenol blue, 50 mM dithiothreitol, and 12.5 mM Tris-HCl, pH 6.8]) were boiled for 10 min. Then, 20 μl was subjected to SDS-PAGE and blotted to polyvinylidene difluoride membranes. Immunodetection was carried out as described previously (Wiese, 1998) with different rabbit or mouse antisera and goat-anti-rabbit or goat-anti-mouse secondary antibodies coupled to horseradish peroxidase (Dianova, Hamburg, Germany) followed by chemiluminescence detection using the Supersignal system (Pierce Chemical, Rockford, IL).

LmxMPK3 Deletion Constructs

To generate the *LmxMPK3* null mutants Δ*LmxMPK3*::*HYG*/Δ*LmxMPK3*::*NEO* and Δ*LmxMPK3*::*PHLEO*/Δ*LmxMPK3*::*NEO* abbreviated Δ1 and Δ2, respectively, *LmxMPK3* and its flanking regions were amplified from a plasmid carrying a DNA-fragment isolated from a genomic DNA library of *L. mexicana* (Wiese *et al*., 1995, 2003b). A PCR was performed on this plasmid (5 min at 94°C, 25 × [30 s at 94°C, 30 s at 50°C, 1 min 45 s at 72°C], 7 min at 72°C, 4°C) using the oligomers 5′-GAGAGGGGGAGGACACTT-3′ and 5′-TGT**GATATC**CTCTTCTCGGCTG-3′, the latter introducing an EcoRV restriction site into the 5′-untranslated region (UTR) of *LmxMPK3*. Because a second EcoRV site is present in the 3′-UTR the amplified fragment was cut using EcoRV and ligated into pBluescriptII SK(+) (Stratagene, La Jolla, CA) previously modified to lack a BspLU11I site and linearized at EcoRV, resulting in pBE5upLmxMPK3ds. To replace *LmxMPK3* by different resistance marker genes BspLU11I and NheI sites were introduced into pBE5upLmxMPK3ds using the oligomers 5′-CTGTGACTGGTG**AGTACT**CAACCAAG-3′ (covering the ScaI site in the β-lactamase gene of the plasmid) and 5′-CTGG**CCTAGG**ACATGTTGGCTACTCTGTGTGC-3′ containing an AvrII and a BspLU11I site in one PCR to amplify the 5′-flanking region, and the oligomers 5′-ATGACTTGGTTG**AGTACT**CACCAGTC-3′ (largely complementary to the ScaI-primer mentioned before) and 5′-CAGG**CCTAGG**CTAGCTAGCGCGCATCTTCTC-3′ containing an AvrII and a NheI site in a second PCR to amplify the 3′-flanking region. The resulting DNA-fragments were trimmed using AvrII and ScaI and ligated to each other, resulting in a plasmid with *LmxMPK3* replaced by BspLU11I, AvrII, and NheI restriction sites. This plasmid was linearized using BspLU11I and NheI and ligated to DNA-fragments carrying the resistance marker genes for the hygromycin B phosphotransferase *HYG*, the neomycin phosphotransferase *NEO*, and the phleomycin binding protein *PHLEO*, prepared as described previously (Benzel *et al*., 2000). The constructs were liberated by EcoRV, gel-purified, and used for electroporation of *L. mexicana* promastigotes in two consecutive rounds as described previously (Bengs *et al*., 2005).

Expression of LmxMPK3 and LmxMKK(D) in Leishmania

For episomal expression of *LmxMPK3* in *L. mexicana*, the open reading frame (ORF) of *LmxMPK3* was amplified using the oligonucleotides 5′-CCAACATGTACAAGAGCAACCAGGAGC-3′ and 5′-GTGAAGCTTCTAGTGATGGTGACCGCT-3′ to introduce BspLU11I and HindIII restriction sites in a PCR (5 min at 94°C, 25 × [30 s at 94°C, 30 s at 45°C, 1 min at 72°C], 7 min 72°C, 4°C) and cloned into pCR2.1TOPO (Invitrogen, Carlsbad, CA) to generate pCR2.1-23MPK3. *LmxMPK3* was released from pCR2.1-23MPK3 using EcoRI and subcloned into MunI of pX63polPHLEO (Wiese, 1998), resulting in pX3ELmxMPK3. This construct was used for transfection of *L. mexicana* promastigotes as described above. Transformants were selected in SDM-79 medium on 96-well tissue culture plates using 5 μg ml^{-1} bleocin.

A 1112-base pair EcoRV/XbaI DNA-fragment was liberated from the pGEX-KG derivative for recombinant expression of LmxMKK(D) generated previously (Wiese *et al*., 2003a) and used for the construction of a plasmid allowing for integration into the ribosomal DNA gene locus as has been described for LmxMKK (Wiese *et al*., 2003a). *LmxMKK* null mutant cells were transfected with 5 μg of a 5.9-kb PacI/PmeI fragment purified from the final construct and recombinants were selected on SDM-79 agar plates containing 20 μM puromycin.

Electron and Light Microscopy and Flagellar Length Determination

For scanning electron microscopy (SEM), *Leishmania* cells were washed twice in PBS, fixed in 2% glutaraldehyde in 0.1 M sodium cacodylate buffer, pH 7.2, and postfixed with 1% OsO_4. Samples were dehydrated at increasing ethanol concentrations (30–100%). After critical point drying, samples were treated with gold and analyzed on a Philips SEM 500 electron microscope. For transmission electron microscopy (TEM), the cells were treated as described for SEM, dehydrated with graded ethanol solutions and propylene oxide. The cells were embedded in an epoxy resin (Epon), and 70-nm ultrathin sections were cut (Ultra Cut E; Reichert/Leica, NuBlock, Germany) and counterstained with uranyl acetate and lead citrate. Sections were examined with a

Philips CM 10 transmission electron microscope at an acceleration voltage of 80 kV. Phase contrast and differential interference contrast (DIC) microscopy and flagellar length determination (the length was measured from the cell surface to the tip of the flagellum using the Openlab software; Improvision, Heidelberg, Germany) were performed on a Zeiss Axioskop 2 Plus and a Leica Leitz DMRB microscope as described previously (Bengs *et al*., 2005).

Recombinant Expression

For recombinant expression of a glutathione *S*-transferase (GST) fusion protein of LmxMPK3, the ORF was liberated from pCR2.1-23MPK3 (see above) with BspLU11I and HindIII, and the DNA-fragment was gel-purified and ligated into the NcoI/HindIII-cleaved pGEX-KG (Guan and Dixon, 1991), resulting in pGEX-KG5aBHLmxMPK3. To generate an enzymatically inactive version of LmxMPK3, lysine 62 was mutated to methionine by site-directed mutagenesis, resulting in LmxMPK3KM. A PCR reaction was performed on pGEX-KG5aBHLmxMPK3 (5 min at 94°C, 25 × [30 s at 94°C, 30 s at 50°C, 45 s at 72°C], 7 min at 72°C, 4°C) using the oligonucleotides 5′-CTATCCCAC-AAATTGATAA-3′ and 5′-TCGCGACACTT**CA**TGATGGACACCTTC-3′. The amplified fragment was cleaved using NruI and XbaI, a 203-base pair fragment isolated and ligated with the 5952-base pair fragment obtained from pGEX-KG5aBHLmxMPK3 cleaved with NruI and XbaI, resulting in pGEX-KG9BHLmxMPK3KM. Both constructs were transformed into *E. coli* XL1-Blue (Stratagene). For expression of the fusion proteins, the bacteria were grown in Luria-Bertani medium, induced with 100 μM isopropyl-α-D-thiogalactopyranoside at an optical density at 600 nm (OD_{600}) of 0.9, further incubated overnight at 18°C, and harvested by centrifugation at 4°C and 4500 × *g* for 15 min. The cells were washed once in cold PBS, resuspended in 50 μl of cold PBS per milliliter of the original culture volume, and the suspension was subjected to sonication on ice with a Branson Sonifier 250 apparatus and a 6-mm tip. The lysate was adjusted to 1% Triton X-100 and end-over-end rotated at 4°C for 1 h. After centrifugation at 4°C and 12,000 × *g* for 10 min, the recombinant proteins were purified on glutathione-Uniflow resin following the instructions of the manufacturer (BD Biosciences, Heidelberg, Germany).

For expression of LmxMKK(D) and LmxMKK(KM) in *E. coli* XL1-Blue, the constructs described previously (Wiese *et al*., 2003a) were used under the same conditions as described for LmxMPK3. To cleave the GST-moiety from the fusion protein, 250 μg of protein was incubated with 0.12 U of thrombin (Amersham, Freiburg, Germany) overnight at 20°C.

Kinase Assay

To determine the interaction of LmxMKK with LmxMPK3, 2 μg of LmxMKK(D) or LmxMKK(K91M) was incubated at 27°C with 2 μg of GSTLmxMPK3 or GSTLmxMPK3(KM) and 0.1 mM [γ-^{32}P]ATP (1000 cpm/pmol) in a volume of 50 μl containing 50 mM 3-(*N*-morpholino)propanesulfonic acid (MOPS), pH 7.0, 10 mM $MnCl_2$, and 0.1 M NaCl. Reactions were terminated after 1 h by the addition of 12.5 μl of 5× SDS sample buffer containing 200 mM dithiothreitol and heating for 10 min at 95°C. Then, 25 μl of the solution was separated on a 12% SDS-PAGE, silver-stained, dried, and exposed to x-ray film at −70°C. For quantification, unlabeled ATP replaced [γ-^{32}P]ATP during the phosphorylation of LmxMPK3 by LmxMKK(D) in a reaction of 20 μl, essentially as described previously (Lawler *et al*., 1997). Then, 350 ng of LmxMKK(D) was incubated with 10 μg of GSTLmxMPK3 at 27°C as described above. After 1 h, 5 μl of this reaction was assayed for GSTLmxMPK3 kinase activity toward MBP at 27°C in a 50-μl reaction containing 50 mM MOPS, pH 7.0, 10 mM $MnCl_2$, 0.1 M NaCl, 1 mM EGTA, 1 mM Na-orthovanadate, 0.3 μg/μl myelin basic protein (MBP), and 0.1 mM [γ-^{32}P]ATP, resulting in an overall molecular ratio of LmxMKK(D)/GSTLmxMPK3/MBP of 1:17:1000. After incubation for 1 h, 40 μl was spotted on phosphocellulose P81 paper (Whatman, Dassel, Germany) and washed four times with 75 mM H_3PO_4 and once with acetone. The papers were air-dried, and the incorporation of phosphate into MBP quantified by Cerenkov counting in a Beckman LS 5000CE liquid scintillation counter.

Phosphoprotein Analysis

For phosphoprotein purification, 2 × 10^9 promastigotes of *L. mexicana* wild-type, ΔLmxMKK−/−, and ΔLmxMKK−/− + LmxMKK(D) were harvested. Before lysis, the cells were washed with 20 mM HEPES, pH 7.5, subsequently lysed in 5 ml of phosphoprotein lysis buffer, and subjected to affinity purification as described by the manufacturer (QIAGEN, Hilden, Germany). The phosphoproteins were collected in five eluates from the affinity column, each with a volume of 500 μl, and the protein concentration determined in a Bradford assay. After elution, the single eluates were incubated at 95°C for 10 min in 1× SDS sample buffer. The samples were subjected to immunoblot analysis with the anti-LmxMPK3-antiserum.

RESULTS

Molecular Characterization

LmxMPK3 is one of nine MAP kinase homologues we identified from *L. mexicana* in a screen using degenerate oligonucleotides encoding highly conserved amino acid regions in subdomains VIb and VIII of MAP kinases (Wiese *et al*., 2003b). The gene is comprised of an open reading frame of 1164 base pairs coding for a protein of 388 amino acids with a calculated molecular mass of 43.7 kDa. Homologues are present in other kinetoplastids, such as *Leishmania major* (98% identical amino acids $^{382}/_{388}$; our unpublished data), *Leishmania infantum* (98% identical amino acids $^{382}/_{388}$; our unpublished data), *Trypanosoma brucei* (70% identical amino acids $^{262}/_{370}$), and *Trypanosoma cruzi* (69% identical amino acids $^{259}/_{373}$). Less homologous, but still significant, are the proteins from *Chlamydomonas reinhardtii* (44% identical amino acids $^{157}/_{350}$), from *Solanum tuberosum* (46% identical amino acids $^{165}/_{356}$), and the ERK1 kinase from *Dictyostelium discoideum* (45% identical amino acids $^{158}/_{351}$; Gaskins *et al*., 1994). The sequence of LmxMPK3 displays the typical 12 kinase subdomains and amino acid residues known to be highly conserved in MAP kinases (Figure 1). There are the subdomain I residues G40–G45 forming the phosphate anchor ribbon for ATP binding with the consensus GxGxxG and the p + 1 specificity pocket in subdomain VIII (I198-R203). In addition, there are the catalytic site residues K62, R76, R79, E80, R160, D161, K163, N166, D179 (Mg^{2+} ligand), R184, T194, D195, and Y196, the latter three forming the TXY motif, which is characteristic for MAP kinases and known to be phosphorylated by the activating MAP kinase kinase on threonine and tyrosine to generate the active enzyme. Lysine 62 in subdomain II is a conserved residue found in all protein kinase family members (Hanks *et al*., 1988) and is essential for catalytic activity (Zoller and Taylor, 1979; Zoller *et al*., 1981; Kamps and Sefton, 1986; Buechler and Taylor, 1989; Gibbs and Zoller, 1991). The potential common docking (CD)-domain (DEEDE), an accumulation of negatively charged residues that is likely to be involved in protein–protein interactions is depicted in Figure 1 (Tanoue and Nishida, 2003). Splice-acceptor sites for *LmxMPK3* were determined using total RNA in a reverse transcriptase-PCR with gene internal and mini-exon primers (see *Materials and Methods*). Amplified fragments were cloned and sequenced. Three AG splice-acceptor sites were found located 58, 61, and 90 base pairs upstream of the ATG translation initiation codon. Interestingly, all three amplification products were found in RNA obtained from lesion-derived amastigotes despite the fact that the mRNA of *LmxMPK3* is down-regulated in this life stage (Wiese *et al*., 2003b). Southern blot analysis of genomic DNA from *L. mexicana* proved that *LmxMPK3* is a single copy gene in the haploid genome (our unpublished data).

Immunoblot Analyses

Using a polyclonal antiserum raised in a rabbit against a carboxy-terminal peptide of LmxMPK3, the protein was readily detectable in a cell lysate of 2 × 10^7 promastigotes, whereas it could not be detected in the same number of amastigotes derived from lesions grown in BALB/c mice after infection with *L. mexicana* wild-type promastigotes (Figure 2). This reflects the above-mentioned down-regulation of *LmxMPK3* mRNA in amastigotes (Wiese *et al*., 2003b). As a control for the presence of comparable amounts of nondegraded protein in each lane, the blot was stripped and treated with a polyclonal antiserum against myo-inositol-1-phosphate synthase, a protein known to be expressed in both life stages (Ilg, 2002). After differentiation of amastigotes to promastigotes using lesion-derived amastigotes to inoculate promastigote growth medium, LmxMPK3 appears within 16–22 h after differentiation initiation (Figure 3A). However, LmxMKK is already detectable in the population

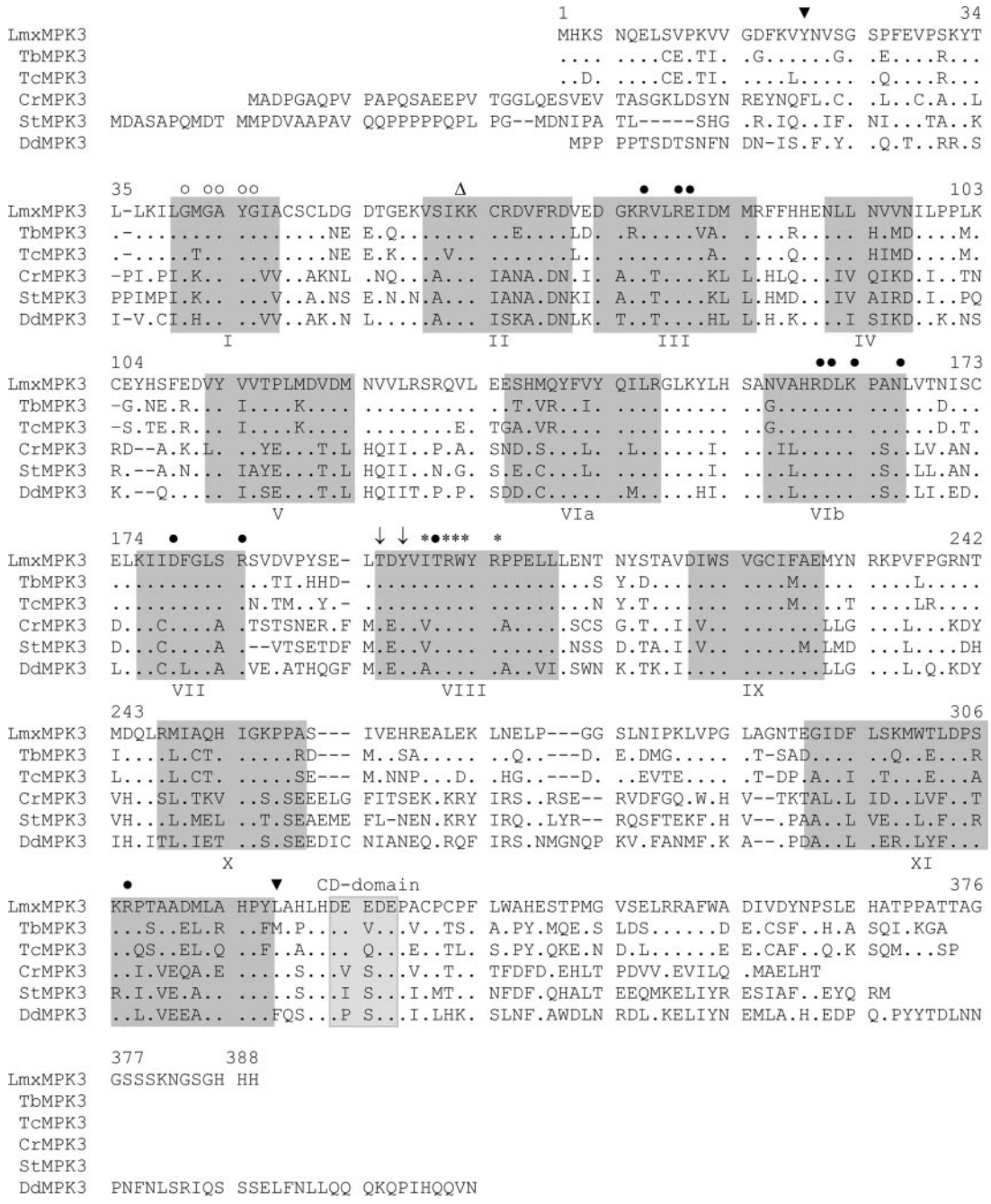

Figure 1. Alignment of LmxMPK3 from *L. mexicana* with MAP kinase amino acid sequences from different species. LmxMPK3, *L. mexicana* MAP kinase 3 (accession no. AJ293281); TbMPK3, *Trypanosoma brucei* MAP kinase 3 (accession no. GeneDB Tb927.8.3550); TcMPK3, *Trypanosoma cruzi* MAP kinase 3 (accession no. GeneDB Tc00.1047053509553.60); CrMPK, *Chlamydomonas reinhardtii* MAP kinase (accession no. AB035141); StMPK2, *Solanum tuberosum* MAP kinase (accession no. AB062138); and DdMPK3, *Dictyostelium discoideum* MAP kinase 3 (accession no. A56042). Roman numerals I to XI indicate kinase subdomains. The kinase domain is located between the two inverted triangles. Arrows mark the potential regulatory phosphorylation sites in the TXY motif at Thr194 and Tyr196, filled circles indicate conserved amino acid residues, and open circles depict the residues of the phosphate anchor ribbon for ATP binding. The asterisks show the residues of the p + 1 specificity pocket. The open triangle marks the invariant lysine residue (Lys62), which is essential for the phosphate transfer reaction. The putative CD-domain is indicated. Dashes indicate gaps introduced to optimize the alignment; dots represent identical residues. Numbering corresponds to LmxMPK3.

after 10 h (Figure 3B). At 19–22 h, most of the cells displayed short flagella not allowing the cells to swim (Figure 3C). At 38 h after differentiation initiation, the cells had flagella of normal length and function. After the in vitro differentiation of promastigotes to amastigotes by pH and temperature shift, the analysis of LmxMPK3 levels by immunoblotting revealed that the amount of protein gradually declines to an amount below the level of detection at 48 h after induction of

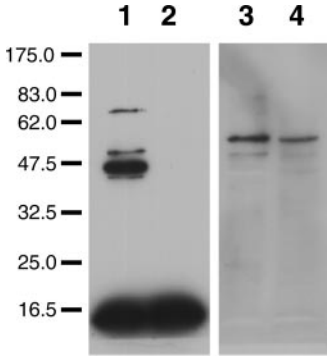

Figure 2. Immunoblot of LmxMPK3 from *L. mexicana* pro- and amastigote total cell lysates. Lanes 1 and 3, 2×10^7 promastigotes; lanes 2 and 4, 2×10^7 lesion-derived amastigotes. Lanes 1 and 2 were probed with antiserum against a COOH-terminal peptide of LmxMPK3; lanes 3 and 4 were probed with antiserum against recombinant myo-inositol-1-phosphate synthase. The molecular masses of standard proteins are indicated in kilodaltons.

differentiation (Figure 3D). During the same time, the cells completely loose their flagella (Figure 3F). For LmxMKK, we observed a slower decline of protein levels with a weak band still present at 72 h (Figure 3E). During this time, the cells adopted the spherical amastigote morphology (Figure 3F).

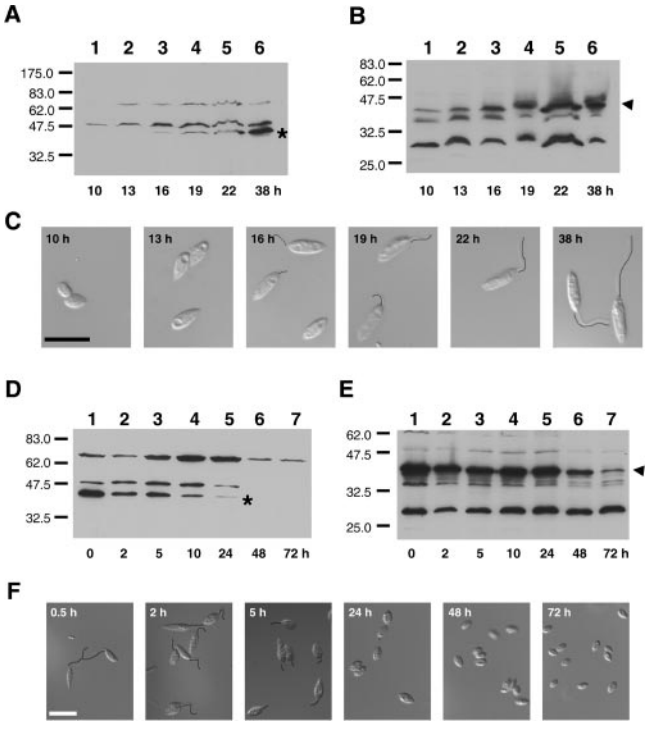

Figure 3. Differentiation of amastigotes to promastigotes (A–C) and promastigotes to amastigotes (D–E). Immunoblots from *L. mexicana* total cell lysates were probed with LmxMPK3 (A and D) and LmxMKK (B and E) antisera. Hours after differentiation initiation are indicated. The molecular masses of standard proteins are given in kilodaltons. The asterisk depicts the bands corresponding to LmxMPK3; the triangle depicts the bands for LmxMKK. C and F, pictures were taken from fixed cells at the indicated time points using DIC microscopy. For better visualization of flagellar lengths, lines were drawn along the flagella. Bar, 10 μm.

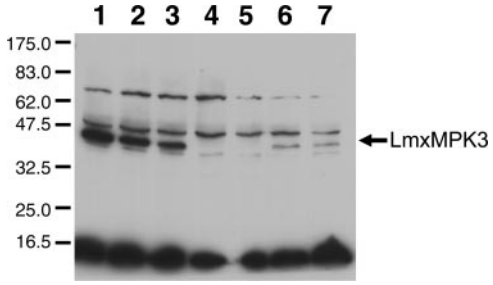

Figure 4. Immunoblot of LmxMPK3 from *L. mexicana* wild type and various mutants. Lane 1, *L. mexicana* wild type; lanes 2 and 3, two independent single-allele knockout mutants; lanes 4 and 5, two null mutants derived from the different single-allele knockouts; and lanes 6 and 7, episomal complementation of the two null mutants. The molecular masses of standard proteins are indicated in kilodaltons.

Targeted Deletion of LmxMPK3 and Complementation

The two alleles of *LmxMPK3* were sequentially replaced by the selective marker genes conferring hygromycin B (*HYG*), G418 (*NEO*), or bleocin (*BLE*) resistance. Targeted replacement of *LmxMPK3* was ensured using 790 base pairs of the 5′-UTR and 652 base pairs of the 3′-UTR of *LmxMPK3* surrounding either of the resistance marker genes. Southern blot analysis of the wild-type, single-allele deletion, and null mutants with probes detecting the *LmxMPK3* wild-type gene locus or the integration of the resistance marker genes revealed the expected bands for accurate replacement (our unpublished data). Immunoblot analysis of total cell lysates from logarithmically growing wild-type, two independent single-allele deletion, and two null mutant promastigotes derived from these single-allele knockouts could not detect the protein in the null mutants and showed a decrease in its amounts in the single-allele deletion mutant (Figure 4). Complementation of the null mutant reintroducing the gene on a plasmid led to reexpression of the protein, albeit in lower amounts (Figure 4, lanes 6 and 7).

The Phenotype of the Null Mutant

The overall appearance of the null mutant promastigotes resembled the appearance of those promastigotes generated by the deletion of *LmxMKK*, the gene for a MAP kinase kinase homologue from *L. mexicana* (SEM; Figure 5) (Wiese *et al*., 2003a). If at all, the cells displayed a flagellum rarely reaching one-half of the length of the wild-type flagellum (Figure 5, A and B). However, as in the LmxMKK null mutant, they were able to wiggle slowly with their flagel-

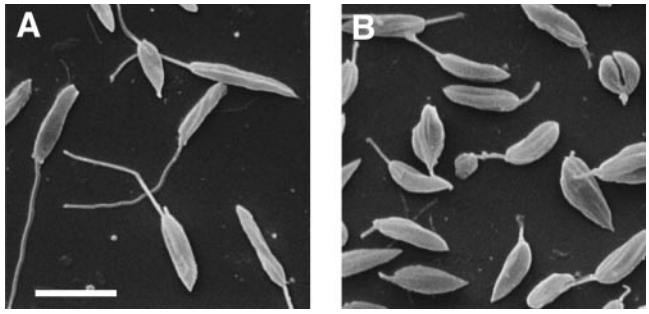

Figure 5. Scanning electron micrograph of *L. mexicana*. Wild type (A) and *LmxMPK3* null mutant (B) promastigotes at the same magnification. Bar, 10 μm.

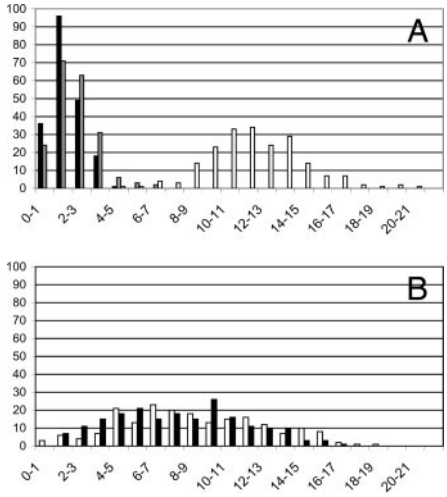

Figure 6. The Δ*LmxMPK3*−/− phenotype. Histograms of flagellar lengths from wild-type and mutant *L. mexicana* promastigotes. The abscissa show groups of flagellar lengths in micrometers; the ordinates indicate the numbers of cells counted. (A) White bars, *L. mexicana* wild type; black bars, Δ*LmxMPK3*−/− clone 1 or Δ1; gray bars, Δ*LmxMPK3*−/− clone 2 or Δ2. (B) White bars, Δ*LmxMPK3*−/− clone 1 + *LmxMPK3* or A1; black bars, Δ*LmxMPK3*−/− clone 2 + *LmxMPK3* or A2.

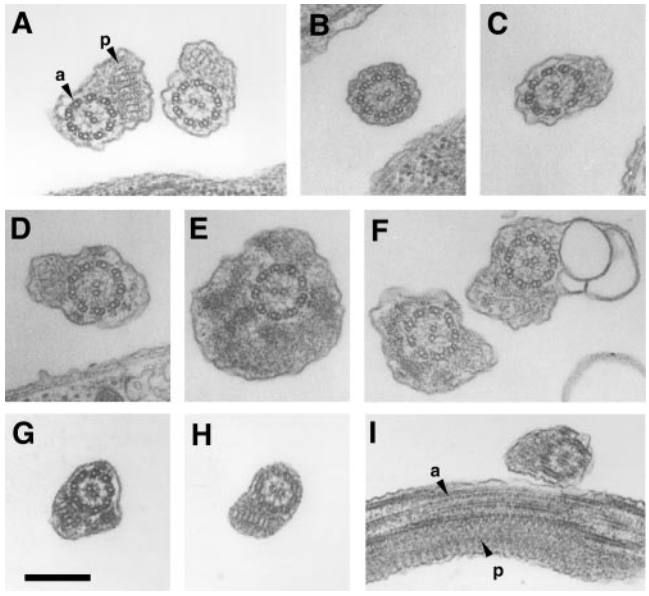

Figure 7. Ultrastructure of *L. mexicana* wild-type and *LmxMPK3* mutant (Δ*LmxMPK3*−/−) flagella. Cross-sections of flagella of chemically fixed *L. mexicana* wild-type promastigote (A), Δ*LmxMPK3*−/− promastigotes (B–F), and episomal complementation (G–I) at the same magnification. a, axoneme; p, paraflagellar rod. Bar, 0.25 μm.

lum, leading to a tumbling locomotion, but keeping the cells at the bottom of the culture flask. The average flagellar length as determined from 400 individual cells depicted randomly from two independent null mutants by phase-contrast microscopy was 2 μm with a size range from 0 to 6.7 μm, whereas the wild type displayed flagella with an average length of 11.8 ± 2.6 μm (Figure 6A). Indeed, the maximal flagellar length differed in the two mutants being 4.6 μm for mutant Δ1 and 6.7 μm for mutant Δ2. The null mutants were complemented by introducing the wild-type *LmxMPK3* cloned into the plasmid pX63polPAC (Bengs *et al*., 2005) (Figure 6B). These cells generated long flagella again; however, the length varied from 1 to 18 μm (average flagellar length of 8.2 ± 3.7 μm), which is likely due to different expression levels generally observed in *Leishmania* harboring an episome (Benzel *et al*., 2000). The ultrastructure of the mutants was analyzed using transmission electron microscopy on chemically fixed cells (Figures 7 and 9). Wild-type flagella showed the typical (9 + 2) pattern of microtubule doublets in the axoneme and the typical lattice-like structure of the paraflagellar rod (PFR) adjacent to the axoneme (Figure 7A). The deletion mutant clones also revealed the typical axoneme; however, the PFR could never be visualized as clear as in the wild type. Instead, different transverse sections could be found either lacking the PFR entirely (Figure 7B), displaying remnants of the PFR (Figure 7C), or various amounts of undefined material around the axoneme (Figures 7, D–F, and 9C), sometimes also displaying vesicles of different size (Figures 7F and 9B). Again, the two null mutants differed from each other. Whereas in the mutant that revealed the longer flagella (mutant Δ2), 17% (34/200) of the transverse sections revealed a PFR at least resembling that of the wild type, no such sections could be observed for the mutant with the shorter flagella (mutant Δ1). Twenty-four percent (48/200) of the sections of mutant Δ2 and 8.5% (17/200) of the mutant Δ1 revealed a rudimentary PFR. No PFR was present in 34% (68/200) of the sections of mutant Δ2 and 29% (58/200) of mutant Δ1. However, mutant Δ1 (61/200; 30.5%) revealed twice as many flagella with material present all around the axoneme as mutant Δ2 (30/200; 15%). Finally, vesicles were present in 10% (20/200) and 32% (64/200) of the flagellar transverse sections for mutant Δ2 and mutant Δ1, respectively. In immunofluorescence analysis, 85% of the mutant promastigotes revealed a fluorescence of varying intensity, 15% showed no reaction with the anti-PFR-2 antibody (our unpublished data). The morphology of the flagella was reflected by a quantification of PFR-2, one of the major protein components of the PFR, by immunoblot analysis (Figure 8). The mutants contain on average roughly 20 times less PFR-2 than the wild type, significantly less than expected, because a mere reduction of flagellar length would only lead to 5 times less PFR-2. In the add-back, small numbers of flagellar sections showed no PFR (15/200), material all around the axoneme (2/200), or vesicles (12/200). A rudimentary PFR was found in 15% (30/200) and a relatively normal architecture of the flagellum in 70.5% (141/200) of the sections, indicating that reexpression of *LmxMPK3* is able to complement the null mutant phenotype. It is interesting to note that in flagellar trans-

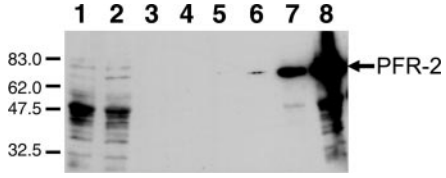

Figure 8. Immunoblot of PFR-2 (mAb L8C4) from *L. mexicana* wild-type and null mutants. Lane 1, Δ*LmxMPK3*−/− Δ1 (2×10^7 promastigotes); lane 2, Δ*LmxMPK3*−/− Δ2 (2×10^7 promastigotes); and lanes 3–8, *L. mexicana* wild-type promastigotes. Lane 3, 5×10^4; lane 4, 1×10^5; lane 5, 5×10^5; lane 6, 1×10^6; lane 7, 5×10^6; and lane 8, 2×10^7. The molecular masses of standard proteins are indicated in kilodaltons.

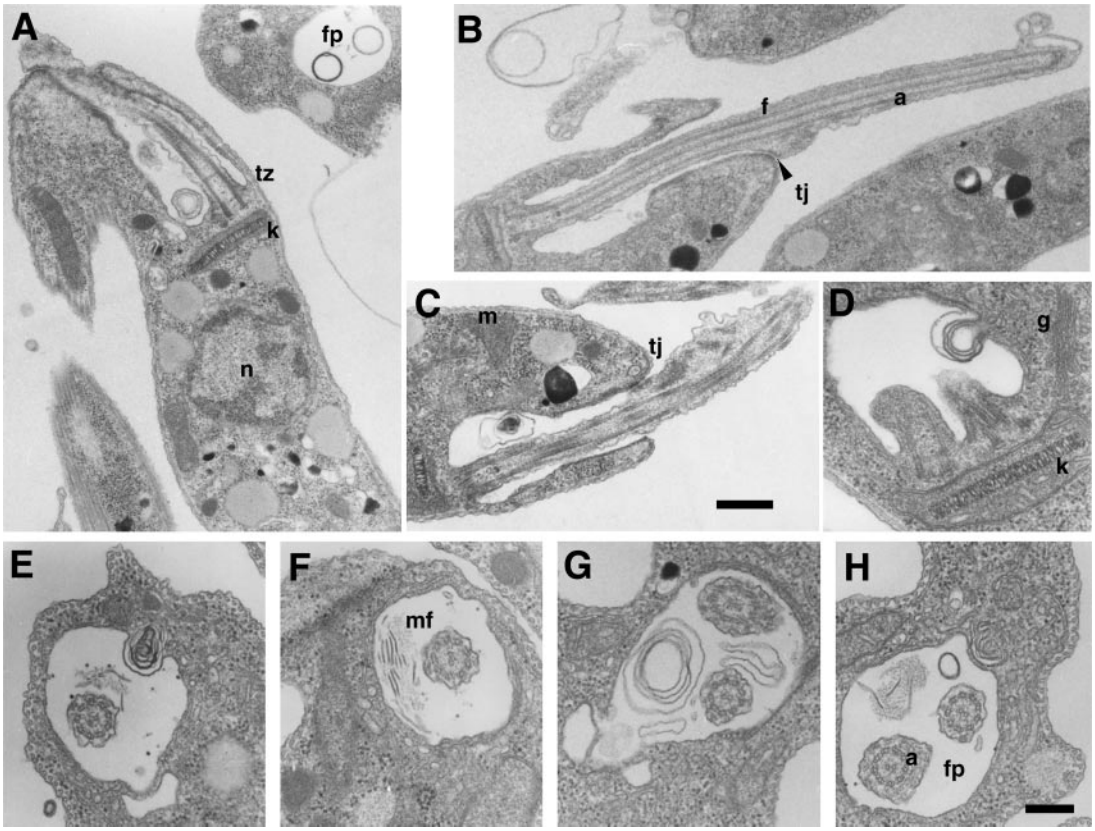

Figure 9. Ultrastructure of *LmxMPK3* null mutant (Δ*LmxMPK3*−/−) cells and flagella. Longitudinal sections of flagellar pockets and flagella of chemically fixed promastigotes. (A) Vesicles with single and double membranes in flagellar pockets. (B) Vesicles at the flagellar tip. (C) Bloated flagellum. (D, E, and G) Multilayered vesicles in flagellar pockets. (E, F, and H) Membrane fragments (mf) in flagellar pockets. a, axoneme; f, flagellum; fp, flagellar pocket; g, Golgi; k, kinetoplast; m, mitochondrium; mf, membrane fragments; n, nucleus; tj, tight junction; tz, transition zone. Bars, 0.5 μm (A–C), 0.25 μm (D–H).

verse sections of the add-backs, the axoneme seemed more condensed (Figure 7, G–I) showing a significantly reduced diameter (~160 nm) compared with the wild type (~180 nm), but the normal cross-hatched structure of the PFR in the longitudinal section of the flagellum (Figure 7I). Indeed, the null mutant showed the most relaxed structure with an axonemal diameter of ~210 nm. As found in the null mutant for *LmxMKK*, we also observed vesicles and membrane fragments in the flagellar pocket of the *LmxMPK3* knockout (Figure 9, A–H). The vesicles revealed single membrane layers (Figure 9, A and H), double layers (Figure 9A), or multiple layers (Figure 9, C–E and G).

L. mexicana wild type, *LmxMPK3* single-allele, null mutants, and episomal add-backs were used to infect female BALB/c mice. No significant differences in the progression of lesion development could be observed between the mutant cell lines and the wild-type (our unpublished data), indicating that LmxMPK3 is neither required for the differentiation from promastigotes to amastigotes nor for the proliferation of the amastigotes.

Recombinant Expression and Kinase Assay

LmxMPK3 and its enzymatically inactive version LmxMPK3(K62M) (Carrera *et al*., 1993) were expressed as glutathione *S*-transferase fusion proteins and found as 71-kDa proteins on SDS-PAGE (Figure 10A, left, lanes 3 and 4). Both proteins were subjected to kinase assays using MBP as an artificial substrate. As expected, only the wild-type protein displayed auto- and substrate-phosphorylation (Figure 10A, right, lanes 3 and 4). Using recombinant GST-LmxMPK3 and MBP in kinase assays under varying conditions revealed that an increase in temperature from 25 to 40°C at 10 mM Mn^{2+}, pH 6.5, led to an increase in auto- and substrate-phosphorylation. Moreover, manganese is preferred over magnesium at promastigote growth temperature of 27°C and pH 6.5. The optimal pH was found to be a pH range from 6.0 to 7.0 at 2 mM Mn^{2+}, 10 mM Mg^{2+}, and 27°C (our unpublished data).

Activation of LmxMPK3 by LmxMKK

Because the promastigotes of the null mutants for *LmxMKK* and *LmxMPK3* both displayed short flagella, it was likely that the two kinases belong to the same signal transduction pathway. To test whether LmxMKK indeed phosphorylates and activates LmxMPK3, the recombinant proteins and their enzymatically inactive versions (LmxMKK(K91M) and LmxMPK3(K62M)) were used in kinase assays. We have shown previously that recombinant wild-type LmxMKK has no autophosphorylation activity (Wiese *et al*., 2003a). Using this protein in an assay to phosphorylate MBP also showed no incorporation of radioactive phosphate into the substrate (our unpublished data). Therefore, we used the constitutively active aspartate mutant LmxMKK(D) in which several residues, including the potential phosphorylation sites of the phosphorylation lip, were replaced by aspartate residues in the activation assay (Wiese *et al*., 2003a). Equal amounts of the two kinases were used with MBP as a substrate, fol-

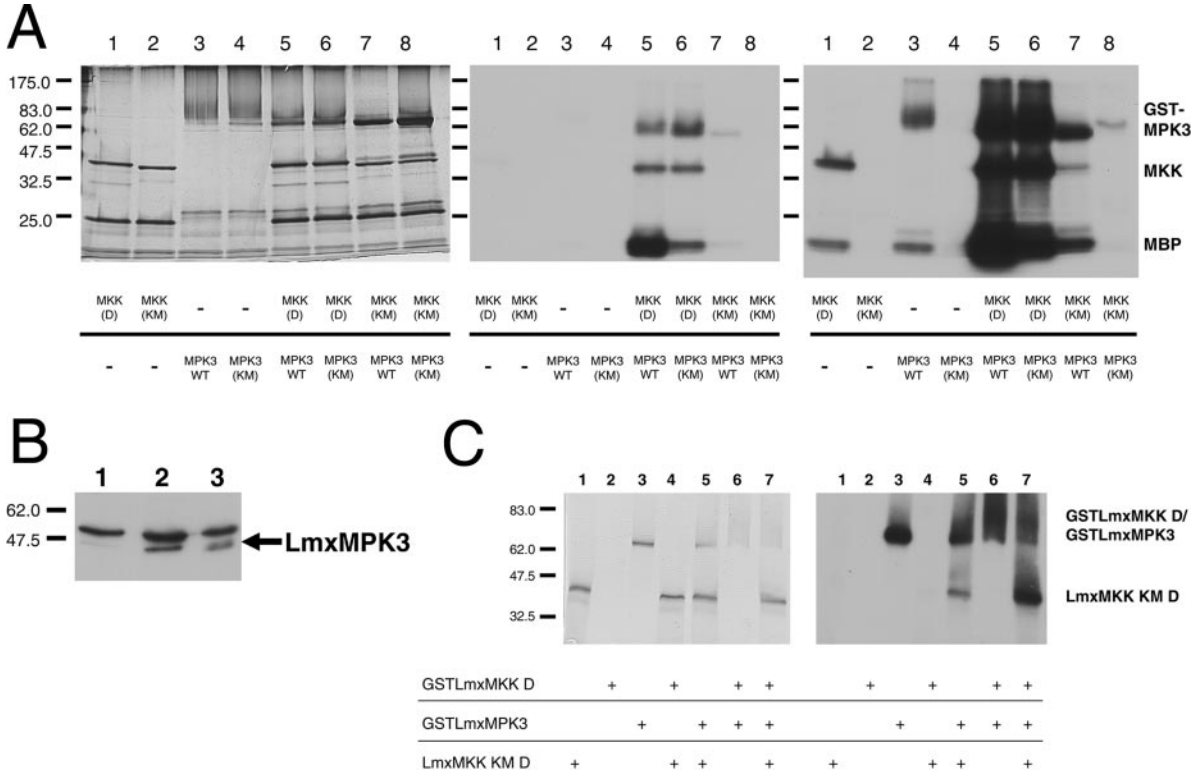

Figure 10. Phosphorylation of LmxMPK3 and LmxMKK. (A) LmxMKK activates LmxMPK3 in vitro. Recombinant kinases were subjected to kinase assays with MBP using 10 mM Mn^{2+}, 50 mM MOPS, pH 7.0, at 27°C either in combination or alone as indicated and resolved by SDS-PAGE followed by autoradiography. Left, silver-stained gel. Middle, autoradiograph of the gel exposed for 6 h. Right, autoradiograph exposed for 5 d. MKK(D), constitutively active aspartate mutant of LmxMKK; MKK(KM), enzymatically inactive mutant of LmxMKK; MPK3 WT, GST-fusion protein of LmxMPK3; MPK3(KM), GST-fusion protein of enzymatically inactive mutant of LmxMPK3. (B) In vivo phosphorylation of LmxMPK3 by LmxMKK. Phosphorylated proteins were enriched from total promastigote cell lysates, subjected to SDS-PAGE, blotted, and LmxMPK3 detected using the polyclonal antiserum against a COOH-terminal peptide. Lane 1, null mutant for *LmxMKK* (Δ*LmxMKK*−/−); lane 2, *L. mexicana* wild type; lane 3, promastigotes expressing LmxMKK(D) from the ribosomal DNA gene locus in Δ*LmxMKK* (Wiese *et al*., 2003a). (C) Feedback phosphorylation of LmxMKK by LmxMPK3. Phosphorylation of an enzymatically inactive version of the aspartate mutant of LmxMKK, designated LmxMKK(KM)(D). Recombinant kinases were subjected to kinase assays either in combination or alone and with or without preincubation with LmxMKK(D) to activate LmxMPK3 as indicated, and resolved by SDS-PAGE. Left, Coomassie-stained gel. Right, autoradiograph of the gel exposed for 6 h. The molecular masses of standard proteins are indicated in kilodaltons.

lowed by SDS-PAGE and autoradiography to visualize the incorporation of radioactive phosphate into the different reaction partners (Figure 10A). To separate LmxMKK(D) from LmxMPK3, the GST-moiety was cleaved off after purification of LmxMKK(D), leading to a mobility of the protein at around 42.5 kDa in SDS-PAGE (Figure 10A, left). The gel was exposed for 5 d to prove that LmxMKK(D) and GSTLmxMPK3 are both capable to perform auto- and substrate-phosphorylation (Figure 10A, right, lanes 1 and 3). Furthermore, the KM-versions of LmxMKK(D) and GSTLmxMPK3 showed no phosphorylation at all (Figure 10A, right, lanes 2 and 4). The constitutively active LmxMKK(D) in combination with GSTLmxMPK3 wild-type reveals the strongest phosphorylation of all three components in the kinase assay already after 6 h of exposure (Figure 10A, middle, lane 5). Especially, MBP phosphorylation is significantly increased. Moreover, LmxMKK(D) and GSTLmxMPK3 show stronger autophosphorylation as in the assay using the proteins on their own. GSTLmxMPK3(K62M) is phosphorylated by LmxMKK(D) (Figure 10A, middle, lane 6) whereas GSTLmxMPK3(K62M) shows no labeling when used on its own (Figure 10A, right, lane 4). MBP is phosphorylated to a higher extent as in the assay using LmxMKK(D) alone (compare Figure 10A, right, lanes 1 and 6), indicating that the interaction with LmxMPK3 increases the activity of LmxMKK. Using LmxMKK(D)(K91M) together with GSTLmxMPK3 also led to a slight increase of the incorporation of labeled phosphate into the MAP kinase and MBP compared with GSTLmxMPK3 alone, but significantly less than in the reaction using additional LmxMKK(D) (compare Figure 10A, right, lane 7 with lanes 3 and 5). Moreover, the GSTLmxMPK3, which has not been activated by LmxMKK(D), not only shows autophosphorylation and phosphorylation of MBP but also phosphorylates LmxMKK(K91M) to some extent, which might indicate feedback regulation (see below). Finally, in the reaction using the two enzymatically inactive kinases residual incorporation of radioactive label into GSTLmxMPK3(KM) could be observed in the long exposure (Figure 10A, right panel, lane 8). Having shown that increased efficiency of MBP phosphorylation depends on the phosphorylation of LmxMPK3 by LmxMKK(D), we quantified the effect caused by the activation of GSTLmxMPK3 with regard to MBP phosphorylation. To preferentially measure MBP phosphorylation by activated GSTLmxMPK3, a method essentially established as described previously was applied (Lawler *et al*., 1997). In an assay with unlabeled ATP to phosphorylate and activate GSTLmxMPK3, 17-fold less molecules of LmxMKK(D) were used compared with GSTLmxMPK3. This reaction was diluted 10-fold into an assay containing [γ-^{32}P]ATP to phosphory-

late MBP. Residual incorporation of labeled phosphate into LmxMKK(D) by autophosphorylation could be neglected due to the saturation of the nonradioactive phosphorylation in the activation reaction (our unpublished data). Moreover, the 17-fold lower amount of LmxMKK(D) compared with GSTLmxMPK3 prevents a significant contribution of the MAP kinase kinase to the phosphorylation of MBP. An increase of MBP phosphorylation of up to 35-fold was obtained by preincubation of GSTLmxMPK3 with LmxMKK(D) compared with GSTLmxMPK3 on its own (our unpublished data). To prove the phosphorylation of LmxMPK3 by LmxMKK in vivo, we enriched phosphorylated proteins from promastigotes of the wild type, the *LmxMKK* null mutant, and cells expressing LmxMKK(D) integrated into the rDNA gene locus in the *LmxMKK* deletion background. The proteins were subjected to SDS-PAGE and immunoblot analysis using the polyclonal antiserum against the carboxy-terminal peptide of LmxMPK3 (Figure 10B). LmxMPK3 was readily detectable among the phosphorylated proteins of wild-type promastigotes (Figure 10B, lane 2). We could not detect any phosphorylated LmxMPK3 in the *LmxMKK* null mutant (Figure 10B, lane 1), whereas in the cells expressing the constitutively active LmxMKK(D) significant amounts of phosphorylated LmxMPK3 were present (Figure 10B, lane 3). Therefore, LmxMPK3 is in the same signal transduction cascade as LmxMKK and likely to be directly phosphorylated by LmxMKK in vivo. However, we cannot exclude the albeit unlikely possibility of additional kinases interposed between LmxMKK and LmxMPK3.

Feedback Phosphorylation

Using 1-h preincubation of GSTLmxMPK3 and GSTLmxMKK(D) as single kinases or together in the presence of ATP followed by an incubation with LmxMKK(K91M)(D), an enzymatically inactive version of the aspartate mutant of LmxMKK, led to the phosphorylation of LmxMKK(K91M)(D) by GSTLmxMPK3 (Figures 10C, lanes 5 and 7). Without activation of LmxMPK3 by LmxMKK(D), the phosphorylation of LmxMKK(K91M)(D) is significantly weaker, indicating that activation of LmxMPK3 by LmxMKK(D) is a prerequisite for full feedback phosphorylation. LmxMKK(K91M)(D) shows no autophosphorylation activity (Figure 10C, lane 1). Likewise, the small amounts of GSTLmxMKK(D) used for the preincubation do not incorporate any label in the radioactive assay (Figure 10C, lane 2). It is interesting to note that GSTLmxMPK3 still reveals high autophosphorylating activity after 1 h of preincubation in the presence of unlabeled ATP (Figure 10C, lane 3). GSTLmxMKK(D) is not able to transphosphorylate LmxMKK(K91M)(D) significantly (Figure 10C, lane 4). The interaction of GSTLmxMKK(D) with GSTLmxMPK3 is reflected by the appearance of a smear in the gel, which is phosphorylated (Figures 10C, lanes 6 and 7). Whether the feedback phosphorylation decreases or augments the activity of LmxMKK has not been investigated yet.

DISCUSSION

We characterized LmxMPK3, a mitogen-activated protein kinase homologue from *L. mexicana*. The protein is exclusively expressed in promastigotes, the insect stage of the parasite, as is LmxMKK, a MAP kinase kinase homologue (Wiese *et al*., 2003a). The stage-specific expression is also reflected by a significant decrease of steady-state mRNA for both genes in *Leishmania* amastigotes (Duncan *et al*., 2001; Wiese *et al*., 2003b). A null mutant for *LmxMKK* displayed short flagella and shorter promastigote cell bodies that revealed membrane fragments and vesicles in their flagellar pockets (Wiese *et al*., 2003a). Indeed, independently generated homozygous deletion mutants of *LmxMPK3* showed a similar phenotype, indicating that the two kinases are components of a common MAP kinase signal transduction pathway involved in the regulation of flagellar length. In wild-type amastigotes, a rudimentary flagellum that lacks the PFR is maintained in the flagellar pocket not protruding from the cell body. As expected PFR-2, a major protein component of the PFR, is not detectable by immunoblot analysis in the amastigote stage of the parasite (Santrich *et al*., 1997). During differentiation from amastigotes to promastigotes, the flagellum is extended and the PFR is assembled next to the axoneme but is restricted to the part of the flagellum outside the flagellar pocket. Although LmxMKK appears within 10 h after initiation of differentiation, LmxMPK3 is first detectable after 16 h. At this time, short flagella are detectable by light microscopy. In contrast, in cells differentiating from promastigotes to amastigotes LmxMPK3 almost disappears within 24 h. LmxMKK is still detectable after 72 h after initiation of differentiation despite the complete reduction of the flagellum within 24 h, indicating that LmxMKK might have additional functions beside the regulation of LmxMPK3 activity. Most importantly, we found that LmxMKK is involved in the phosphorylation of LmxMPK3 in vivo. No phosphorylated LmxMPK3 could be detected in promastigotes lacking LmxMKK, whereas promastigotes expressing the constitutively active LmxMKK showed phosphorylated LmxMPK3 like the wild type. Autophosphorylation of LmxMPK3 in vivo seems to play a minor role, if at all. Regulatory molecules such as the two kinases obviously have to be present before effector molecules such as PFR-2 and other structural components of the flagellum are expressed and assembled. Indeed, PFR-2 is first detectable after at least 25 h after promastigote differentiation initiation (our unpublished data). At this time, most of the cells already displayed short flagella resembling those of the two kinase null mutants. Interestingly, in the *LmxMKK* null mutant most of the cells showed no PFR-2 in immunofluorescence analysis, whereas up to 85% of the *LmxMPK3* null mutant promastigotes revealed variable amounts of PFR-2 in their flagella (our unpublished data). However, as revealed by electron microscopy PFR-2 was not properly assembled into the lattice-like structure as in the wild type. This indicates that LmxMKK might be a branch point in the regulation of flagellar morphogenesis and has other substrates in addition to LmxMPK3, which are responsible for the expression of PFR-2, whereas LmxMPK3 might affect the assembly of the PFR. MAP kinase kinases exhibit high levels of substrate specificity (Chang and Karin, 2001); however, yeast Ste7 phosphorylates Kss1 and Fus3, MKK7 phosphorylates different isoforms of SAPK1/JNK1 and p38 (Fleming *et al*., 2000), and mitogen-activated protein kinase kinase 1 phosphorylates extracellular signal-regulated kinase (ERK)1, ERK2, and a potential Golgi-associated ERK (Acharya *et al*., 1998). A regulatory motif of 10 nucleotides responsible for a 10-fold down-regulation of the amount of mRNA in the amastigote has been identified in the 3′-UTR of all PFR genes in *L. mexicana* (Mishra *et al*., 2003). This element could not be found in the 3′-UTRs of *LmxMKK* and *LmxMPK3*. The proposed additional substrate of LmxMKK might be a MAP kinase that phosphorylates an RNA-binding protein that then stabilizes PFR mRNA, leading to the expression of PFR proteins. LmxMPK3, in contrast, might be involved in the regulation of the IFT, supporting the outgrowth of the flagellum and the proper assembly of the PFR because the null mutants never display its cross-hatched structure. Whether the activity of kinesin II, the molecular motor driving anterograde IFT, is regulated by phosphory-

lation has not been investigated yet; however, potential MAP kinase phosphorylation sites have been identified in both motor proteins forming at least part of the kinesin II complex in *Leishmania* (Wiese, unpublished data).

Using recombinant proteins, we could demonstrate that LmxMPK3 is phosphorylated by a constitutively active LmxMKK, leading to an increase in phosphorylation of the artificial substrate MBP by the activated LmxMPK3. Moreover, the activated LmxMPK3 was able to phosphorylate its activator, revealing a potential feedback mechanism that might either lead to an increase in kinase activity, inactivate the kinase, or mark it for degradation. Higher eukaryotic Cdc2 kinase and its regulating molecules are examples for different roles of phosphorylation. Negative phosphorylation by Wee1 and Myt1 during interphase inactivates Cdc2. At the onset of mitosis Cdc2 is dephosphorylated by Cdc25 phosphatase which in turn is phosphorylated by Cdc2, increasing its phosphatase activity. Active Cdc2 also phosphorylates its inhibitory kinase Wee1, generating a phospho-degron (signal for degradation). This is recognized by an E3 ubiquitin-ligase, thereby targeting Wee1 for proteasome-dependent degradation, thus preventing inactivation of Cdc2 (Watanabe *et al*., 2004). Provided that LmxMPK3 behaves like a typical MAP kinase and displays a substrate specificity for serine or threonine followed by a proline residue, there are two potential phosphorylation sites in LmxMKK, serine 117 and threonine 279. It has yet to be tested whether they are indeed phosphorylated to influence the activity or half-life of LmxMKK.

The LmxMKK-LmxMPK3 cascade is not restricted to kinetoplastids because a homologue for LmxMPK3 was found in the flagellated green alga *Chlamydomonas reinhardtii*. Preceding mitosis the two flagella of *Chlamydomonas* are resorbed and grow again once the cell has completed division (Cavalier-Smith, 1974). The LmxMPK3 homologue might be involved in the regulation of the outgrowth of the new flagellum in the daughter cells. Although flagellar resorption is coupled to the differentiation to amastigotes in *Leishmania*, it is likely to be coupled to cytokinesis in *Chlamydomonas*. *Leishmania* might have lost this feature because the promastigotes are attached to the wall of the gut of the sandfly by inserting their flagellum between the microvilli of the gut. Resorption of the flagellum before cytokinesis would detach the cell and bear the risk of being excreted with the feces. Nevertheless, *Leishmania* needs to have a mechanism to initiate the formation of a new flagellum next to the old flagellum before cytokinesis. This cannot be the LmxMKK-LmxMPK3 signaling cascade because amastigotes without expressing the two kinases form a new flagellum before cell division with the difference that it never extends beyond the cell surface. In promastigotes, this mechanism allows for the growth of a short flagellum, lacking an appropriately assembled PFR. A full-length flagellum can only be formed in the presence of both kinases. Because *Chlamydomonas* lacks a PFR, the regulation of PFR assembly in *Leishmania* is likely to be an additional function beside the elongation of the flagellum. Indeed, PFR null mutants display full-length flagella (Maga *et al*., 1999).

The possibility to activate LmxMPK3 will facilitate the identification of the substrate(s) of this kinase, which could either be a gene regulatory molecule affecting components involved in the elongation and maintenance of the flagellum or components of the IFT itself. Now, we have reached a level very close to the elucidation of the regulation of gene expression in an organism lacking RNA polymerase II promoters and the usual eukaryotic transcription factors.

ACKNOWLEDGMENTS

We thank Andrea MacDonald for expert technical assistance, Keith Gull (University of Oxford, Oxford, United Kingdom) for providing monoclonal antibody L8C4, and Thomas Ilg (Max-Planck-Institute for Biology, Tuebingen, Germany) for the anti-myo-inositol-1-phosphate synthase antiserum.

REFERENCES

Aboagye-Kwarteng, T., Ole-MoiYoi, O. K., and Lonsdale-Eccles, J. D. (1991). Phosphorylation differences among proteins of bloodstream developmental stages of *Trypanosoma brucei brucei*. Biochem. J. *275*, 7–14.

Acharya, U., Mallabiabarrena, A., Acharya, J. K., and Malhotra, V. (1998). Signaling via mitogen-activated protein kinase kinase (MEK1) is required for Golgi fragmentation during mitosis. Cell *92*, 183–192.

Bengs, F., Scholz, A., Kuhn, D., and Wiese, M. (2005). LmxMPK9, a mitogen-activated protein kinase homologue affects flagellar length in *Leishmania mexicana*. Mol. Microbiol. *55*, 1606–1615.

Benzel, I., Weise, F., and Wiese, M. (2000). Deletion of the gene for the membrane-bound acid phosphatase of *Leishmania mexicana*. Mol. Biochem. Parasitol. *111*, 77–86.

Berman, S. A., Wilson, N. F., Haas, N. A., and Lefebvre, P. A. (2003). A novel MAP kinase regulates flagellar length in *Chlamydomonas*. Curr. Biol. *13*, 1145–1149.

Brun, R., and Schoenenberger, M. (1979). Cultivation and in vitro cloning of procyclic culture forms of *Trypanosoma brucei* in a semi-defined medium. Acta Trop. *36*, 289–292.

Buechler, J. A., and Taylor, S. S. (1989). Dicyclohexylcarbodiimide cross-links two conserved residues, Asp-184 and Lys-72, at the active site of the catalytic subunit of cAMP-dependent protein kinase. Biochemistry *28*, 2065–2070.

Carrera, A. C., Alexandrov, K., and Roberts, T. M. (1993). The conserved lysine of the catalytic domain of protein kinases is actively involved in the phosphotransfer reaction and not required for anchoring ATP. Proc. Natl. Acad. Sci. USA *90*, 442–446.

Cavalier-Smith, T. (1974). Basal body and flagellar development during the vegetative cell cycle and the sexual cycle of *Chlamydomonas reinhardtii*. J. Cell Sci. *16*, 529–556.

Chang, L., and Karin, M. (2001). Mammalian MAP kinase signalling cascades. Nature *410*, 37–40.

Dell, K. R., and Engel, J. N. (1994). Stage-specific regulation of protein phosphorylation in *Leishmania major*. Mol. Biochem. Parasitol. *64*, 283–292.

Duncan, R., Alvarez, R., Jaffe, C. L., Wiese, M., Klutch, M., Shakarian, A., Dwyer, D., and Nakhasi, H. L. (2001). Early response gene expression during differentiation of cultured *Leishmania donovani*. Parasitol. Res. *87*, 897–906.

Fleming, Y., Armstrong, C. G., Morrice, N., Paterson, A., Goedert, M., and Cohen, P. (2000). Synergistic activation of stress-activated protein kinase 1/c-Jun N-terminal kinase (SAPK1/JNK) isoforms by mitogen-activated protein kinase kinase 4 (MKK4) and MKK7. Biochem. J. *352*, 145–154.

Gaskins, C., Maeda, M., and Firtel, R. A. (1994). Identification and functional analysis of a developmentally regulated extracellular signal-regulated kinase gene in *Dictyostelium discoideum*. Mol. Cell. Biol. *14*, 6996–7012.

Gibbs, C. S., and Zoller, M. J. (1991). Rational scanning mutagenesis of a protein kinase identifies functional regions involved in catalysis and substrate interactions. J. Biol. Chem. *266*, 8923–8931.

Guan, K. L., and Dixon, J. E. (1991). Eukaryotic proteins expressed in *Escherichia coli*: an improved thrombin cleavage and purification procedure of fusion proteins with glutathione S-transferase. Anal. Biochem. *192*, 262–267.

Hanks, S. K., Quinn, A. M., and Hunter, T. (1988). The protein kinase family: conserved features and deduced phylogeny of the catalytic domains. Science *241*, 42–52.

Harper, J. D., Sanders, M. A., and Salisbury, J. L. (1993). Phosphorylation of nuclear and flagellar basal apparatus proteins during flagellar regeneration in *Chlamydomonas reinhardtii*. J. Cell Biol. *122*, 877–886.

Ilg, T. (2002). Generation of myo-inositol-auxotrophic *Leishmania mexicana* mutants by targeted replacement of the myo-inositol-1-phosphate synthase gene. Mol. Biochem. Parasitol. *120*, 151–156.

Kamps, M. P., and Sefton, B. M. (1986). Neither arginine nor histidine can carry out the function of lysine-295 in the ATP-binding site of p60src. Mol. Cell. Biol. *6*, 751–757.

Lawler, S., Cuenda, A., Goedert, M., and Cohen, P. (1997). SKK4, a novel activator of stress-activated protein kinase-1 (SAPK1/JNK). FEBS Lett. *414*, 153–158.

Maga, J. A., Sherwin, T., Francis, S., Gull, K., and Lebowitz, J. H. (1999). Genetic dissection of the *Leishmania* paraflagellar rod, a unique flagellar cytoskeleton structure. J. Cell Sci. *112*, 2753–2763.

Marshall, W. F., and Rosenbaum, J. L. (2001). Intraflagellar transport balances continuous turnover of outer doublet microtubules: implications for flagellar length control. J. Cell Biol. *155*, 405–414.

McConville, M. J., and Ferguson, M. A. (1993). The structure, biosynthesis and function of glycosylated phosphatidylinositols in the parasitic protozoa and higher eukaryotes. Biochem. J. *294*, 305–324.

Menz, B., Winter, G., Ilg, T., Lottspeich, F., and Overath, P. (1991). Purification and characterization of a membrane-bound acid phosphatase of *Leishmania mexicana*. Mol. Biochem. Parasitol. *47*, 101–108.

Mishra, K. K., Holzer, T. R., Moore, L. L., and Lebowitz, J. H. (2003). A negative regulatory element controls mRNA abundance of the *Leishmania mexicana* paraflagellar rod gene PFR2. Eukaryot. Cell *2*, 1009–1017.

Mukhopadhyay, N. K., Saha, A. K., Lovelace, J. K., Da Silva, R., Sacks, D. L., and Glew, R. H. (1988). Comparison of the protein kinase and acid phosphatase activities of five species of *Leishmania*. J. Protozool. *35*, 601–607.

Parsons, M., Carter, V., Muthiani, A., and Murphy, N. (1995). Trypanosoma congolense: developmental regulation of protein kinases and tyrosine phosphorylation during the life cycle. Exp. Parasitol. *80*, 507–514.

Parsons, M., Valentine, M., and Carter, V. (1993). Protein kinases in divergent eukaryotes: identification of protein kinase activities regulated during trypanosome development. Proc. Natl. Acad. Sci. USA *90*, 2656–2660.

Parsons, M., Valentine, M., Deans, J., Schieven, G. L., and Ledbetter, J. A. (1991). Distinct patterns of tyrosine phosphorylation during the life cycle of *Trypanosoma brucei*. Mol. Biochem. Parasitol. *45*, 241–248.

Piperno, G., Huang, B., Ramanis, Z., and Luck, D. J. (1981). Radial spokes of *Chlamydomonas* flagella: polypeptide composition and phosphorylation of stalk components. J. Cell Biol. *88*, 73–79.

Piperno, G., and Luck, D. J. (1976). Phosphorylation of axonemal proteins in *Chlamydomonas reinhardtii*. J. Biol. Chem. *251*, 2161–2167.

Santrich, C., Moore, L., Sherwin, T., Bastin, P., Brokaw, C., Gull, K., and Lebowitz, J. H. (1997). A motility function for the paraflagellar rod of *Leishmania* parasites revealed by PFR-2 gene knockouts. Mol. Biochem. Parasitol. *90*, 95–109.

Tanoue, T., and Nishida, E. (2003). Molecular recognitions in the MAP kinase cascades. Cell Signal. *15*, 455–462.

Tuxhorn, J., Daise, T., and Dentler, W. L. (1998). Regulation of flagellar length in *Chlamydomonas*. Cell Motil. Cytoskeleton *40*, 133–146.

Watanabe, N., Arai, H., Nishihara, Y., Taniguchi, M., Watanabe, N., Hunter, T., and Osada, H. (2004). M-phase kinases induce phospho-dependent ubiquitination of somatic Wee1 by SCFbeta-TrCP. Proc. Natl. Acad. Sci. USA *101*, 4419–4424.

Wiese, M. (1998). A mitogen-activated protein (MAP) kinase homologue of *Leishmania mexicana* is essential for parasite survival in the infected host. EMBO J. *17*, 2619–2628.

Wiese, M., Ilg, T., Lottspeich, F., and Overath, P. (1995). Ser/Thr-rich repetitive motifs as targets for phosphoglycan modifications in *Leishmania mexicana* secreted acid phosphatase. EMBO J. *14*, 1067–1074.

Wiese, M., Kuhn, D., and Grunfelder, C. G. (2003a). Protein kinase involved in flagellar-length control. Eukaryot. Cell *2*, 769–777.

Wiese, M., Wang, Q., and Gorcke, I. (2003b). Identification of mitogen-activated protein kinase homologues from *Leishmania mexicana*. Int. J. Parasitol. *33*, 1577–1587.

Zilberstein, D., and Shapira, M. (1994). The role of pH and temperature in the development of *Leishmania* parasites. Annu. Rev. Microbiol. *48*, 449–470.

Zoller, M. J., Nelson, N. C., and Taylor, S. S. (1981). Affinity labeling of cAMP-dependent protein kinase with p-fluorosulfonylbenzoyl adenosine. Covalent modification of lysine 71. J. Biol. Chem. *256*, 10837–10842.

Zoller, M. J., and Taylor, S. S. (1979). Affinity labeling of the nucleotide binding site of the catalytic subunit of cAMP-dependent protein kinase using p-fluorosulfonyl-[14C]benzoyl 5′–adenosine. Identification of a modified lysine residue. J. Biol. Chem. *254*, 8363–8368.